A Molecular Dynamics Investigation of the Elastomeric Restoring Force in Elastin

Z. R. WASSERMAN and F. R. SALEMME

E. I. du Pont de Nemours & Co., Inc., Central Research and Development Department, Experimental Station, P.O. Box 80228, Wilmington, Delaware 19880-0228

SYNOPSIS

A repetitive polypentapeptide organized as a connected chain of β-bends is believed to be an important structural element of elastin, the major elastomer in biological systems. Molecular dynamics simulations were carried out on hydrated polymers of $(Val\text{-}Pro\text{-}Gly\text{-}Val\text{-}Gly)_{18}$ at various extensions. Analysis of the fluctuations of backbone angles in relaxed elastin showed that particularly large-amplitude torsional motions occur in ϕ and ψ angles of residues connecting sequentially adjacent hairpin bends. Many such motions reflect peptide plane librations that result from anticorrelated crankshaft rotations of ψ_i and ϕ_{i+1}. These effects were much reduced in stretched polymer models. The conformational entropy of relaxed and stretched elastin models was estimated using a treatment due to Meirovitch, and gave a calculated decrease in entropy of about 1 cal/mol deg when the polymer was stretched to 1.75 times its original length. There are large changes in solvent-accessible surface area during the initial stages of elastin stretching. Collectively these results suggest that hydrophobic interactions make contributions to elastin entropy at low extensions, but that librational mechanisms make larger contributions to the elastic restoring force at longer extensions.

INTRODUCTION

Elastin is a major bioelastomer characterized by the occurrence of a repetitive pentapeptide sequence $(Val\text{-}Pro\text{-}Gly\text{-}Val\text{-}Gly)_n$ where n is between 10 and 13.[1-3] Although thermoelasticity studies of both natural elastin and synthetic elastin polypentapeptides indicate the elasticity to be entropic in origin, the molecular origins of the entropy differences between relaxed and stretched polymer remain unclear. Flory's classical treatment of polymer elasticity,[4] for example, suggests that conformational entropy differences between the stretched and unstretched states of a polymer provide the major component of the elastic restoring force. In the simplest terms, this theory suggests that stretched molecules are more structurally organized, more conformationally regular, and have reduced flexibility, relative to the unstretched polymers. However, experiments with both natural and synthetic elastin polymers[5-10] show that they undergo a thermal ordering transition between 20 and 40°C that correlates with an increase in polymer elastic modulus.[11-17] This association of increased elastic restoring force and increased polymer order appears contrary to expectations of the simple conformational entropy model.

Urry has proposed a resolution of this paradox that is based upon a librational entropy mechanism of elasticity. This mechanism stems from molecular mechanics studies of a model pentapeptide polymer $(Val\text{-}Pro\text{-}Gly\text{-}Val\text{-}Gly)_n$ that is structurally organized as a continuous coil of β-turns interconnected by glycine residues. The fundamental concept is that the elastomeric restoring force originates from reduction of librational entropy in the tripeptides Val-Gly-Val linking successive β-turns as the elastin coil is stretched. This was investigated by comparative studies of the conformational flexibility of relaxed and extended elastin models. Under conditions where all pentamers but one were fixed, the accessible amplitudes of torsional libration in the residues

CCC 0006-3525/90/12-131613-19 $04.00
Biopolymers, Vol. 29, 1613–1631 (1990)

bridging the bends were reduced as the structure was extended, suggesting that the elasticity arose from a decrease in the number of accessible low-energy conformations.

An alternative mechanism attributes the entropy changes in elastin to the solvent entropy associated with changing hydrophobic surface area of the polymer as it is stretched.[18,19] Stretching is postulated to increase hydrophobic side-chain exposure to the aqueous environment, thereby decreasing the entropy of surrounding waters that are assumed to be relatively immobilized in the vicinity of hydrophobic surfaces. In this model, the elastomeric restoring force arises from the same hydrophobic forces that stabilize folded protein structures.

The present work describes an analysis of elastin elasticity based on computer simulations of polymer molecular dynamics in the relaxed and stretched states in aqueous solvent. Although in vacuo simulations of an elastin polymer have been described previously,[20] the present work samples a wider range of alternative coil geometries at several degrees of extension, and additionally provides the basis for semiquantitative estimates of differences in conformational entropy of the stretched and relaxed polymer chains.

METHODS

This investigation was undertaken in two stages. In the first stage, molecular dynamics simulations were carried out to define initial and incrementally stretched structures of the polymer (Figure 1). Conformational data accumulated from these runs were averaged to produce regular models used as input for the second phase of the work. The second set of simulations, four in all, was performed for the purpose of comparing the dynamic conformational properties of the polymer and estimating its entropy in various stretched states.

Initial Structure

The study was initiated with a rexamination of the relaxed β-spiral model proposed by Urry.[21] This model was derived from an x-ray crystal structure of the cyclic pentadecapeptide (Val-Pro-Gly-Val-Gly)$_3$.[22] The cyclic molecule is organized as 3 type II β-turns, each stabilized by a hydrogen bond between $Val_1(C{=}O)$ and $Val_4(N{-}H)$, linked together by interconnecting residues Gly_5. The cyclic pentadecamers form threefold symmetric, cylindrical stacks in the crystal. The Urry model of the elastin

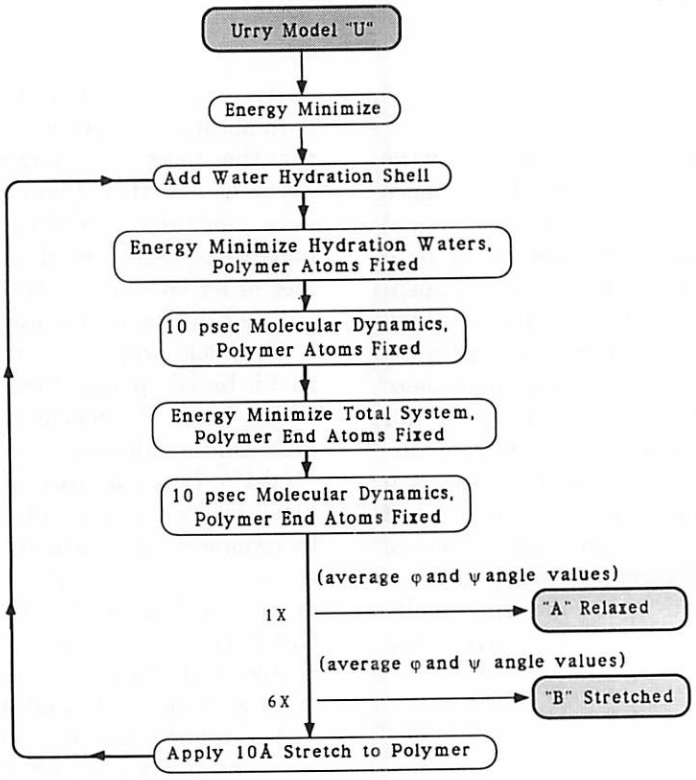

Figure 1 Schematic diagram of the protocol used to produce averaged regular models of relaxed and stretched elastin polymers. See text for additional details.

Table I Helical Parameters, Energy, and Entropy

	Rise per Pentapeptide (Å)	Pentapeptides per Turn	Pitch (Å/turn)	Energy per Residue[a] (kcal)	Entropy per Residue* (cal/mole deg)		
					$b = 0$	$b = 1$	$b = 2$
Urry	3.36	2.73	9.18	−2.4			
C	2.92	3.00	8.75	−3.1	18.1	17.5	17.1
A	3.74	2.97	11.10	−2.0	18.0	17.4	17.1
D	5.10	2.99	15.24	−2.5	17.0	16.4	16.2
B	5.53	2.34	12.95	−1.8	18.3	17.7	17.3

[a] Energies were calculated for the 90-residue molecule in vacuo using a distance-dependent dielectric. Entropies were calculated from a simulation at 300 K in an 8 Å shell of water with a dielectric constant of 1.0, using only the dihedral angle variations of ϕ and ψ of the central eight pentapeptides to evaluate the entropy. These values should not be combined to calculate the free energy.

polymer is produced by a decyclization, lock-washer dislocation, and connection of successive pentadecamers in a crystal stack, to produce a continuous coil of β-turns interconnected by glycine residues. Refinement of this "linear correlate of the cyclic molecule" by a conformational search procedure[21] produced a minimum energy structure corresponding to a right-handed coil with 2.7 pentapeptides per turn and other parameters outlined in Table I. The persistance of this or a related coil structure in solution is supported by the similarity in nmr solution spectra for the cyclic pentadecamers and linear polymers,[23] which both indicate the preservation of the type II β-turns seen in the crystal structure.[22,24]

Initial Structure Relaxation

We carried out initial molecular dynamics simulations of the Urry structure to relieve any strains that might be present and to investigate alternative coil geometries. In particular, it was desirable to allow free variation of polymer helical parameters in order to evaluate relaxed or extended structures that might differ from the 2.7 pentapeptides per turn of the Urry coil model. Since we wanted to simulate the behavior of a structure within the environment of a long polymer chain, simulations were carried out on models with fixed terminal atoms that incorporated 18 pentapeptide units (90 residues). Conformational and statistical data for analysis were accumulated only from the 8 central pentapeptide units. Natural elastin is highly hydrated and contains about 60% water by weight. Accordingly, the simulations incorporated an explicit hydration shell model as described below.

The computations were carried out using the program AMBER[25] with the united atom force field,[26] in which only hydrogen atoms that can potentially participate in hydrogen bonds are explicitly included. As described in Figure 1, the Urry model was initially subjected to 4000 steepest descent energy minimization steps in vacuuo using a distance-dependent dielectric $\epsilon = 1/r_{ij}$. The model was then embedded in a box of water, the result of a computer simulation using the TIP3P potential.[27] Water molecules for which the distance from the oxygen to a protein atom was less than the sum of their respective van der Waals radii, or that were further than 8 Å from all protein atoms, were deleted. The number of waters required to hydrate the relaxed Urry structure was 1526, but ranged between 1244 and 1681 for other states described below. The system hydration shell was subjected to 2000 steps of conjugate gradient minimization with the polymer atoms constrained, followed by 10 ps of molecular dynamics of the waters only. The entire system was then energy minimized for 2000 steps, followed by 10 ps of molecular dynamics with only the end atoms constrained, run at 300 K.

Stretching Protocol

After the initial 10 ps of dynamics simulation, the structure was "instantaneously" stretched 10 Å by proportionally translating all atoms out from the center of mass in a direction parallel to the helix axis. The solvent shell was then minimized and relaxed with 10 ps of molecular dynamics, followed by minimization of the total system and an additional 10 ps of molecular dynamics with fixed polymer end atoms. Relaxing the waters while holding the protein fixed after each "stretch" allowed the waters to reorient around the protein, damping the large motions that might result from bond and bond angle

strain effected by extending the structure in this artificial manner. The cycle of extension–relaxation was carried out 6 times, until the radius of gyration was 1.5 times that of the starting model.

Regularized Models

The sequence of structures obtained by the stretching procedure was not regular, a behavior similar to that observed by Prabhakaran and Harvey in their studies of B-DNA deformation.[28] Some irregularity is probably expected for an open structure like elastin on the time scale of the simulation. However, describing the various stretched structures in terms of average helical parameters provides a useful means of comparing them, and provides a reference state for averaging conformational states in the statistical mechanical estimation of entropy described below. Regular elastin models were built from the first (most contracted) and seventh (most extended) 10 ps periods of the "stretching" simulation trajectory. Values for each of the 10 pentapeptide ϕ and ψ backbone angles were calculated by averaging over the eight symmetry-related central pentapeptide units, as well as over time, in each of the two 10-ps windows. Regular 90-residue elastin models were then built using the averaged ϕ and ψ values, standard bond lengths and angles from the AMBER data base, and *trans* peptide bonds. The conformation derived from the first 10 ps will henceforth be denoted model A, and that from the last (seventh) 10 picoseconds model B. The structures are shown in Figures 2 and 3a, and helical parameters given in Table I.

In the course of this work, we noted that the axial separation between turns was 10 Å in the crystal stacks of cyclic pentadecapeptides, and 9.2 and 11.1 Å respectively, for the helical Urry structure and model A. We also noted that whereas the cyclic molecules have threefold symmetry and model A has approximate threefold symmetry, the Urry structure and model B contain a nonintegral number of pentapeptide units per turn. Since structures with only slight perturbations from threefold symmetry appear to best preserve features of the crystalline cyclic pentadacamer that might optimally stabilize triple-strand coil structures (as postulated to occur for natural elastin[29]), we used interactive graphics and energy minimization to search for other low-energy threefold symmetric models. Two additional structures, models C (contracted) and D (extended), were selected for further study (Figures 2 and 3b and Table I).

Dynamics Simulation

For purposes of analysis, each of the regular model structures A, B, C, and D was energy minimized in vacuo (using a distance-dependent dielectric model), hydrated, solvent relaxed, and then the total system equilibrated by 10 ps of molecular dynamics at each of the temperatures 100, 200, and 300 K. Temperature was maintained by weak coupling to a thermal bath, using the method of Berendsen et al.[30] In the present case atomic velocities were rescaled at each integration step with a time coupling constant τ_T of 0.1 ps. All runs used a 9.5 Å cutoff for the nonbonded interactions and a dielectric constant of 1.0 in simulations that explicitly included water. The integration time step was 1 fs and trajectory points were saved every 50 steps, corresponding to a minimum time interval of 0.05 ps between observed "events." The end atoms were constrained during the simulations and statistical data for analysis accumulated only from the 8 central pentapeptide units.

After the initial 30 ps equilibration periods, simulations of structures A and B were run for 100 ps and C and D for 60 ps. Analysis was carried out only for the part of the simulation after the initial 30 ps equilibration. The simulations were carried out on the CRAY-XMP/24 at the Du Pont Experimental Station, and the analysis on a Digital Equipment VAX 8800. Computer graphics, which were used for initial model building and for examination of trajectories, used the program MOLEDITOR.[31]

Entropy Computation

Entropy was calculated using a procedure due to Meirovitch[32] and a modified version of his program. Meirovitch has calculated the conformational entropy of decaglycine based on rigid geometry Monte Carlo simulations in which the sole degrees of freedom were the backbone angles ϕ and ψ. Since these angles play the major role in determining protein conformation, this method should provide a reasonable first approximation to the entropy even when the simulation has all degrees of freedom enabled. The entropy S is given as

$$S = -k_B \int \rho(\theta_N) \ln \rho(\theta_N) d\theta_N \qquad (1)$$

where the integral is over all conformational space, $\rho(\theta_N)$ is the probability of the structure's being in a conformation with the set of backbone dihedral angles $\{\theta_N\} = [\phi_1, \psi_1, \ldots, \phi_n, \psi_n]$, and $d\theta_N = d\phi_1 d\psi_1 \cdots d\phi_n d\psi_n$.

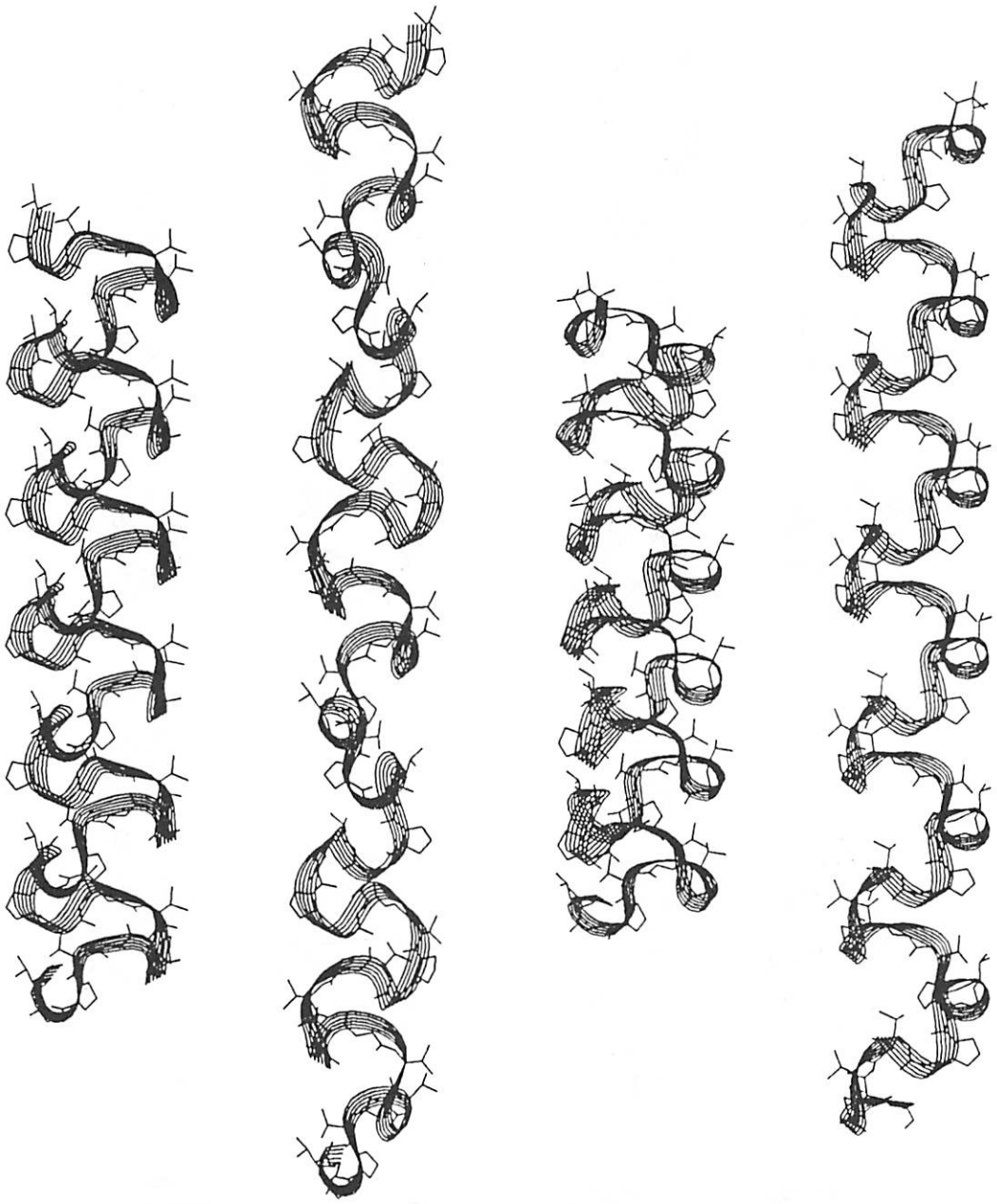

Figure 2 Models A, B, C, and D of the elastin polypentapeptide Val-Pro-Gly-Val-Gly. Each model contains eighteen pentapeptides, a total of 90 residues. The models were built using standard bond lengths and bond angles, *trans* peptide bonds, and side-chain dihedral angles from the AMBER data base. For A and B, main-chain dihedral angles ϕ and ψ were obtained by calculating the average values from a 10-ps segment of a molecular dynamics simulation in which the structure was periodically extended in the direction of the helix axis; only the eight central pentapeptide repeats were used in calculating the averages. C and D were generated using interactive graphics techniques. A and C correspond to relaxed states, B and D to extended. Helix parameters are given in Table I.

Each pentapeptide unit, at each point of the saved simulation trajectory, was considered an independent conformation of the pentapeptide "molecule." To calculate the probabilities ρ, the range of values adopted by each dihedral i is divided into L subranges or boxes. For each conformation, m_i represents the state of the ith dihedral angle, and is assigned a value between 1 and L (we used $L = 12$).

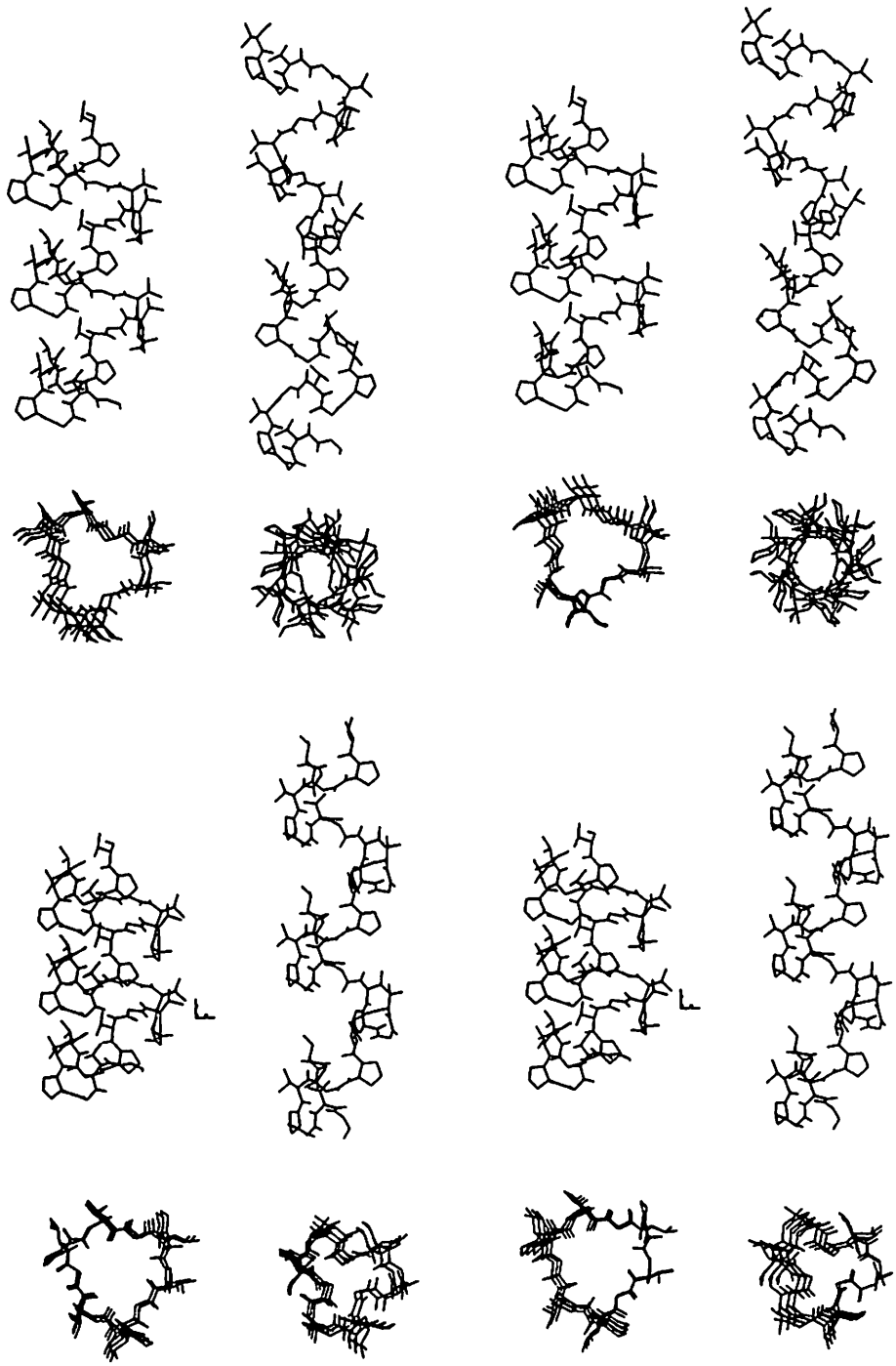

Figure 3 Stereo pair longitudinal and axial views of eight-pentapeptide segments of the polypentapeptide models. (a) Models A and B; (b) models C and D.

The probability that the molecule (or in our case, pentapeptide) is in a conformation θ_N, with dihedral angles in the states represented by m_N, is the product of the probabilities of the individual angles being in states m_i. Since the angles are not independent, each individual probability is the conditional probability that angle i is in state m_i, given that the previous $i - 1$ angles are in states $m_1 \cdots m_{i-1}$.

As an approximation, only the b previous angles were used in calculating the conditional probabilities. Then

$$\rho(\theta_i|\theta_{i-1}, \ldots, \theta_{i-b}) = \frac{n(m_i, m_{i-1}, \ldots, m_{i-b})}{n(m_{i-1}, \ldots, m_{i-b})} \quad (2)$$

where $n(m_i \cdots m_{i-b})$ is the number of pentapeptide

conformations in the dynamics trajectory that have angles $i, \ldots, i - b$ in states $m_i, \ldots, m_{i-b}$, and

$$\rho(\theta_N) = \Pi\rho(\theta_i|\theta_{i-1}, \ldots, \theta_{i-b}) \quad (3)$$

Following Meirovitch, we used $b = 1$ and $b = 2$ in our calculations. For comparison we also calculated the $b = 0$ case, which considers the angles to be independent, with the formula

$$\rho(\theta_i) = \frac{n(m_i)}{N_{\mathrm{TRJ}} \cdot 8} \quad (4)$$

where N_{TRJ} is the number of trajectory points used in the calculation and the factor of 8 accounts for the number of pentapeptide repeats used in the averaging. All the saved trajectory points, representing every 50th step of the simulation, were used in these calculations. Individual pentapeptides occurring in the same time step and those in different time steps were treated in an identical manner.

RESULTS

Large-Scale Motions

Molecular dynamics runs were carried out on all four structures under the conditions described in the Methods section. Inspection of "movies" of the trajectories revealed the occurrence of relatively large-scale motions in the structures. In contrast to most globular proteins, which tend to be organized over long distances by extended hydrogen bonding in secondary structures, the successive hairpin bends characterizing the elastin spirals are more loosely connected, so that each of the structures developed some curvature during the course of the simulation. This was more pronounced for structures B and D than for the more compact structures A and C. The rms deviation of coordinates from average values was greater for both stretched structures than for the relaxed ones. In several of the simulations similar high rms deviations were found for groups of amino acids 15 residues apart, indicating concerted motion of the atoms on one side of the spiral in consecutive turns.

Figure 4 shows the rms deviations from average coordinates during each 15 ps period of simulation D. The dominant feature in the first period is the correlated behavior described above, with greatest motion around residues 35, 50, and 65, and least motion on the opposite side of the spiral. In the second period the greatest motion is in the Pro-Gly pairs of β-bends at residues 43–44 and 63–64. In the third period the motion is reduced and more evenly distributed, and in the fourth period it is sharply reduced. The conformation at the end of 60 ps, showing the curvature that has developed, is shown in Figure 5.

Backbone Angle Motions

Although long-range deformations tend to be larger for the extended structures than for the relaxed ones, analysis of the more localized fluctuations in main-chain dihedral angles shows rather different behavior. In the simulation of the extended model D, for example, the variation in individual torsional angles is considerably reduced relative to the relaxed states. Table II lists the rms deviation from average values of each of the backbone angles ϕ, ψ, and ω in simulations C and D. Averages and deviations were calculated for the eight central pentapeptide repeats, taking successive pentapeptides as independent conformations. The ω's vary within about 10° of 180, consistent with the conformational space spanned by the ω's in protein crystal structures. Proline ϕ's and ψ's also have small rms deviations, reflecting the restricted conformational freedom of this amino acid. The angular fluctuations are concentrated in the ϕ's and ψ's of Val_1, Gly_3, Val_4, and Gly_5.

Local State Multiplicity and Crankshaft Motions

The type of motion that is occurring is elucidated by tracking the time evolution of individual torsional angles. Figures 6a–d plot the ten pentapeptide backbone angles ϕ and ψ for simulations A, B, C, and D, respectively. In each subplot eight curves (corresponding to the eight central pentapeptide units) are overlaid. The enhanced variability exhibited in Figure 6a and c over that of Figure 6d is apparent. The existence of multiple local conformational states is indicated by the clustering of curves around two or more favored angular values. Most often equivalent dihedral angles in different pentamers of the polymer maintain an orientation in either of the favored states throughout the simulation, yet there is evidence of shifting between conformational states.

For example, the ψ of Gly_{35} (the fifth residue of a pentapeptide unit) undergoes a rotation of about −90° at time 54 ps (Figure 7). At almost the same time, ϕ Val_{36} undergoes a rotation of almost the same magnitude in the opposite direction. We found numerous instances of such rotational pairs, always involving ψ_i and ϕ_{i+1}, in the simulations. They occurred more often, and were of greater magnitude, in simulations A and C than in D (B is discussed

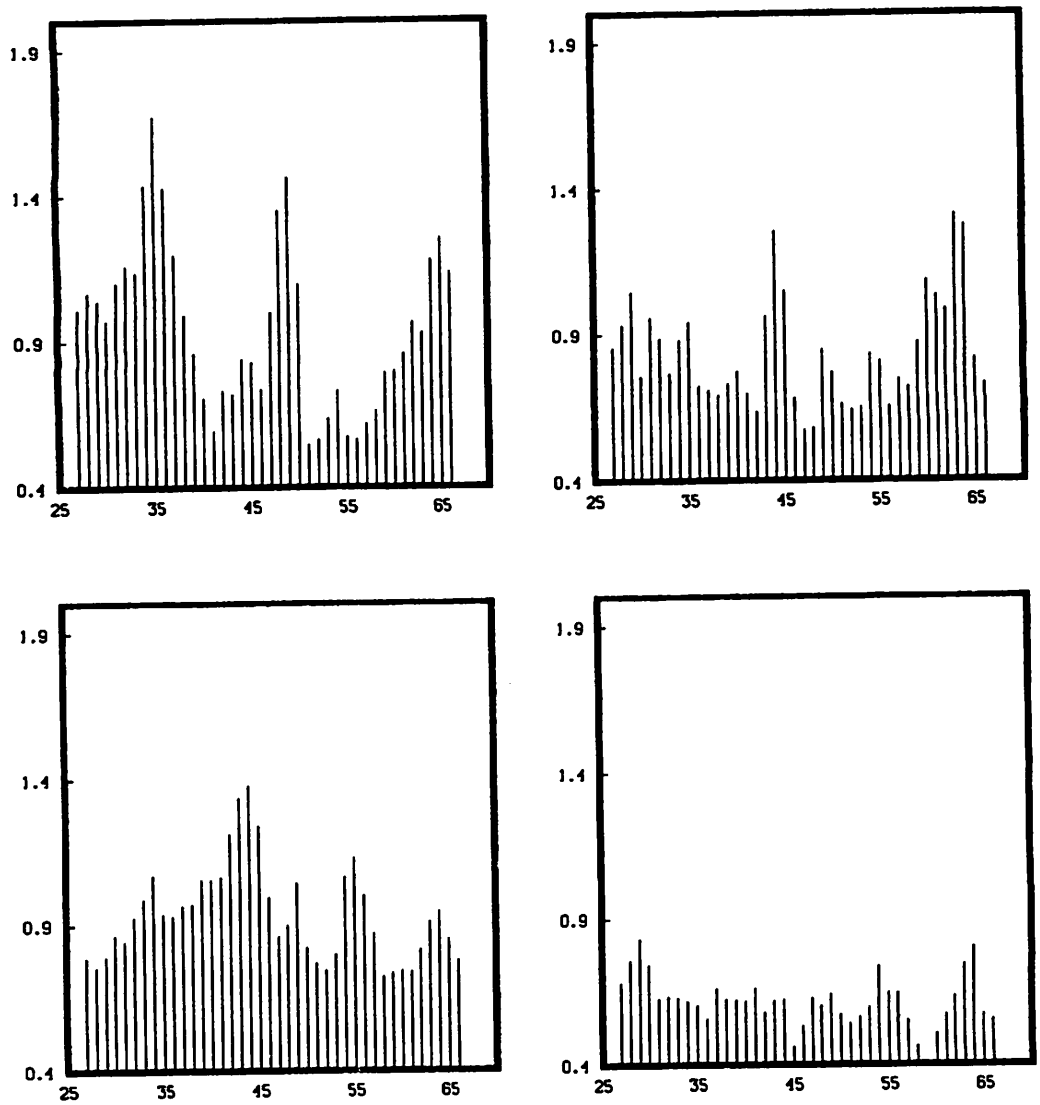

Figure 4 Root mean square atomic fluctuations (Å) averaged over each residue from 15 ps segments of molecular dynamics simulation D. Only backbone atoms were used in computing the fluctuations. (a) Picoseconds 30–45, (b) Picoseconds 45–60, (c) Picoseconds 60–75, and (d) Picoseconds 75–90.

below). This type of crank-like motion, a correlated counterrotation of bonds separated by a *trans* central bond, has been postulated to occur in DNA[33] and proteins,[34] and is prominent in Brownian dynamics simulations of polyethylene.[35,36] It results in a reorientation of the central bond (in this case the peptide bond) with little deformation of the structure on either side of the two rotating bonds, maintaining the overall integrity of the structure.

The simulation of structure B differs in many respects from the others. Although simulations A, C, and D showed occasional transient formation of alternative Gly_3 C=O to Gly_5 NH and Pro_2 C=O to Val_4 NH backbone hydrogen bonds, the Val_1 C=O to Val_4 NH interactions that stabilized the hairpin bends remained essentially intact during the simulation. This was not the case for simulation B where two of the central β-bends disappeared within 100 ps. Not surprisingly, this behavior was accompanied by considerably more variation in backbone angles than in any of the other simulations. Although there were some occurrences of correlated counterrotations of ψ_i and ϕ_{i+1}, there were in addition large changes in the values of some dihedral angles without compensating counterrotations of neighboring angles, causing large deviations from the starting structure. For example, ϕ Gly_{40} undergoes a gradual rotation of over 120°, while ψ Val_{39} fluctuates within

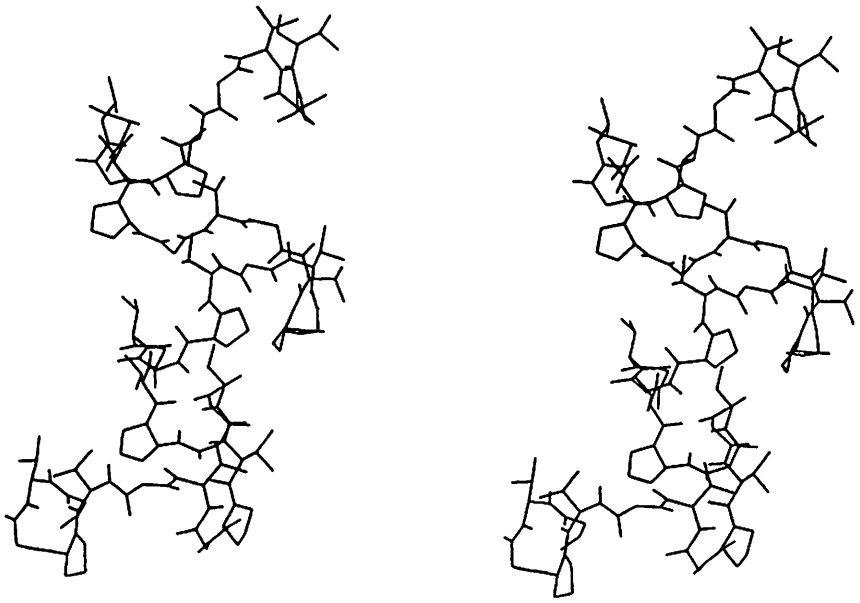

Figure 5 Stereo pair representation of the central eight pentapeptide units of simulation D at time 90 ps. Despite the overall deformation causing substantial curvature local structure has changed comparatively little. All eight Val-Pro-Gly-Val segments remain in β-bend conformation.

a 40° interval (Figure 8). B is the starting conformation of highest energy, the most extended, and the only one without approximate threefold rotational symmetry. For reasons we discuss below, we feel that instability of structure B probably results from a strained starting conformation for which the local potential well is neither deep nor broad.

Entropy Estimates

We attempted to quantify these apparent conformational entropy differences using the procedure outlined in Methods (see Table I). The calculated conformational entropy is approximately equal for simulations A and C and for D is approximately 1 cal/mol deg lower. The entropy of system B, however, is about .3 entropy units greater than that of either A or C. The entropy decreases with increasing values of b (increased accuracy of the calculation), but the entropy differences remain consistent for all values of b.

Table II RMS Deviations of Dihedral Angles from Average Values

	Conformation C			Conformation D		
	ϕ	ψ	ω	ϕ	ψ	ω
Val-1	28.8	13.8	11.9	23.1	10.4	8.9
Pro-2	11.4	17.9	12.0	13.8	16.3	10.2
Gly-3	30.3	28.0	10.9	19.6	35.0	10.5
Val-4	24.0	23.3	10.6	22.0	10.7	11.8
Gly-5	39.0	49.3	10.4	16.9	25.4	10.4

It is of interest to estimate the contribution of crank-like motions to the distribution of conformational states, and hence the conformational entropy, of the elastin polymer. Suppose we consider, for the moment, a highly idealized system containing only two rotatable bonds each of which may occur, with equal probability, in the two states s1 and s2. If the motions of the two bonds were uncorrelated we would have the distribution of states given by the probability matrix of Figure 9a. Calculating the entropy using Eqs. (1)–(3) ($b = 1$) yields the same result as a calculation using Eqs. (1), (4), and (3) ($b = 0$). If, on the other hand, the motion of the two bonds were anticorrelated we would have the probability matrix of Figure 9b. The probability of an individual bond's being in either state remains 1/2 but the distribution of states for the system as a whole is very different. In this case the $b = 0$ approximation, which does not account for correlation, yields a much higher entropy value than $b = 1$, and the difference between the two values is an indication of the extent of correlation between the rotations of the bonds.

Since entropy is additive, the contributions to the entropy due to conformations of individual angles

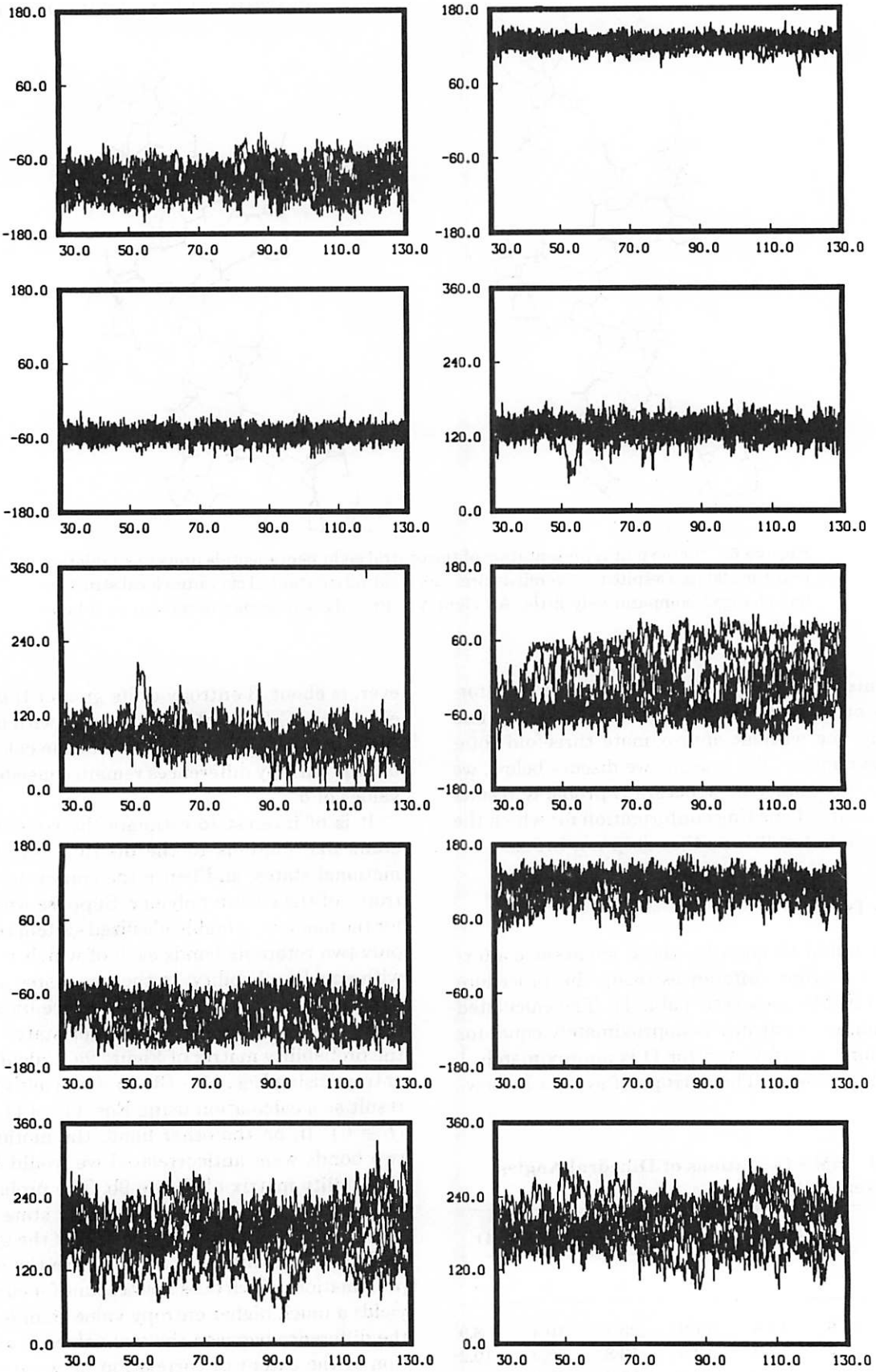

Figure 6 Histories of the backbone dihedral angles ϕ and ψ for Val_1 (top row) through Gly_5 (bottom row). The ϕ values are plotted in the left-hand column and ψ values on the right. In each graph eight curves, corresponding to the eight central pentapeptide units, are overlaid. Correlated motions involve the angle plotted in the right column of one row

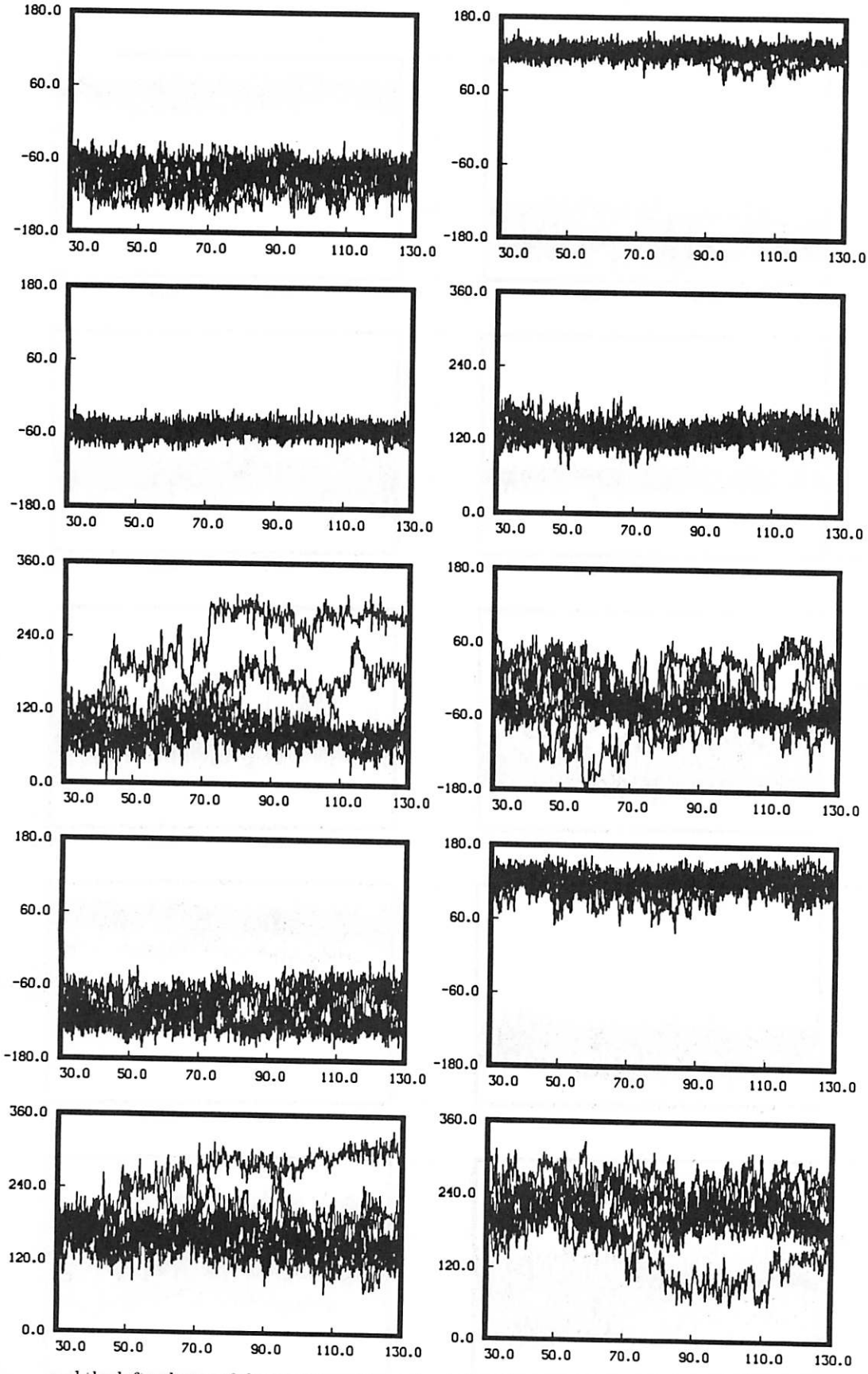

and the left column of the row beneath, or the right column of row five and the left column of row one. (a) Simulation A, (b) B, (c) C, and (d) D. Each graph depicts a 360° range, but in order to avoid discontinuities some plots have been centered at 0° and others at 180°. The x axis is time in picoseconds.

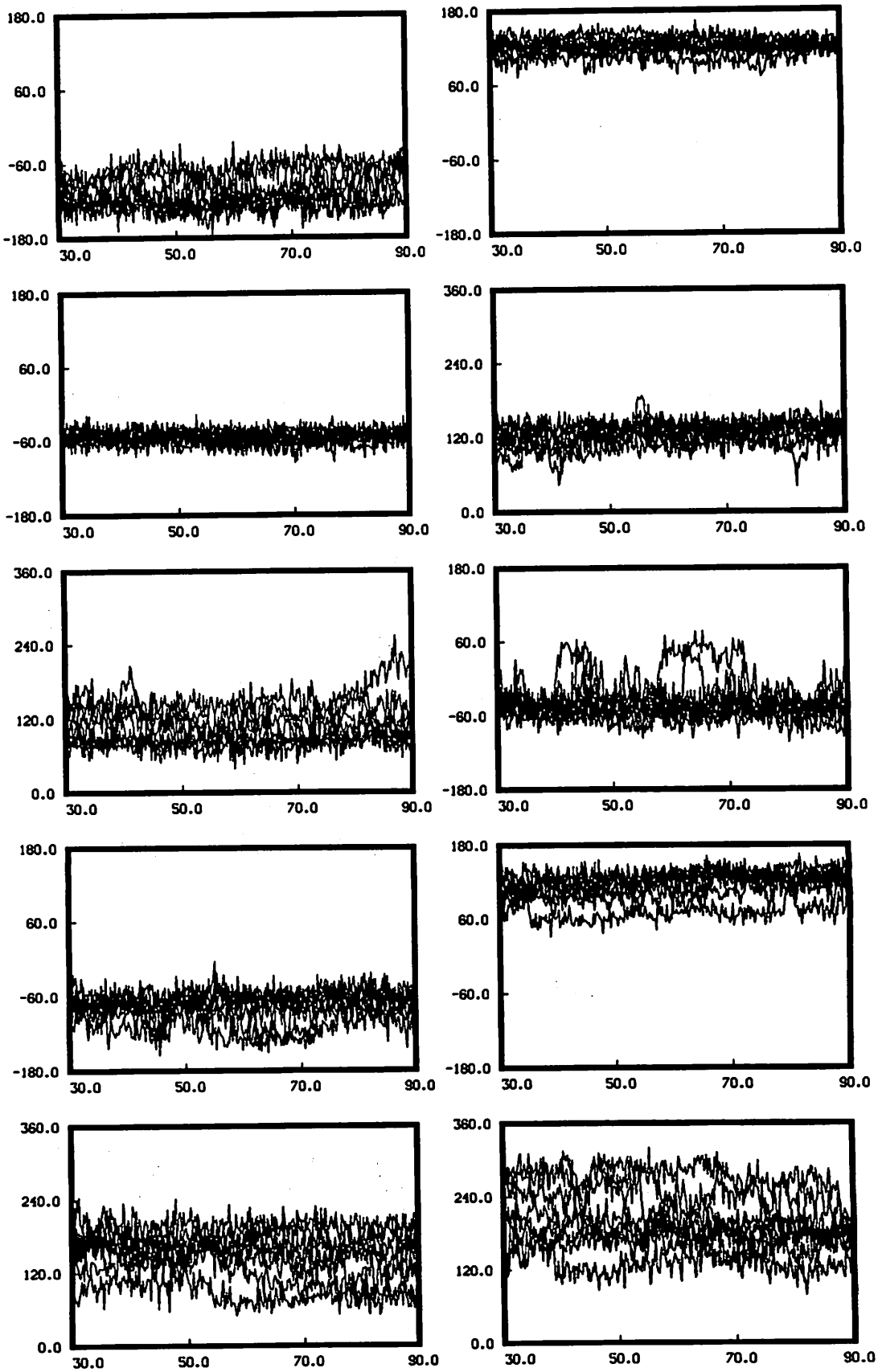

Figure 6. *(Continued from the previous page.)*

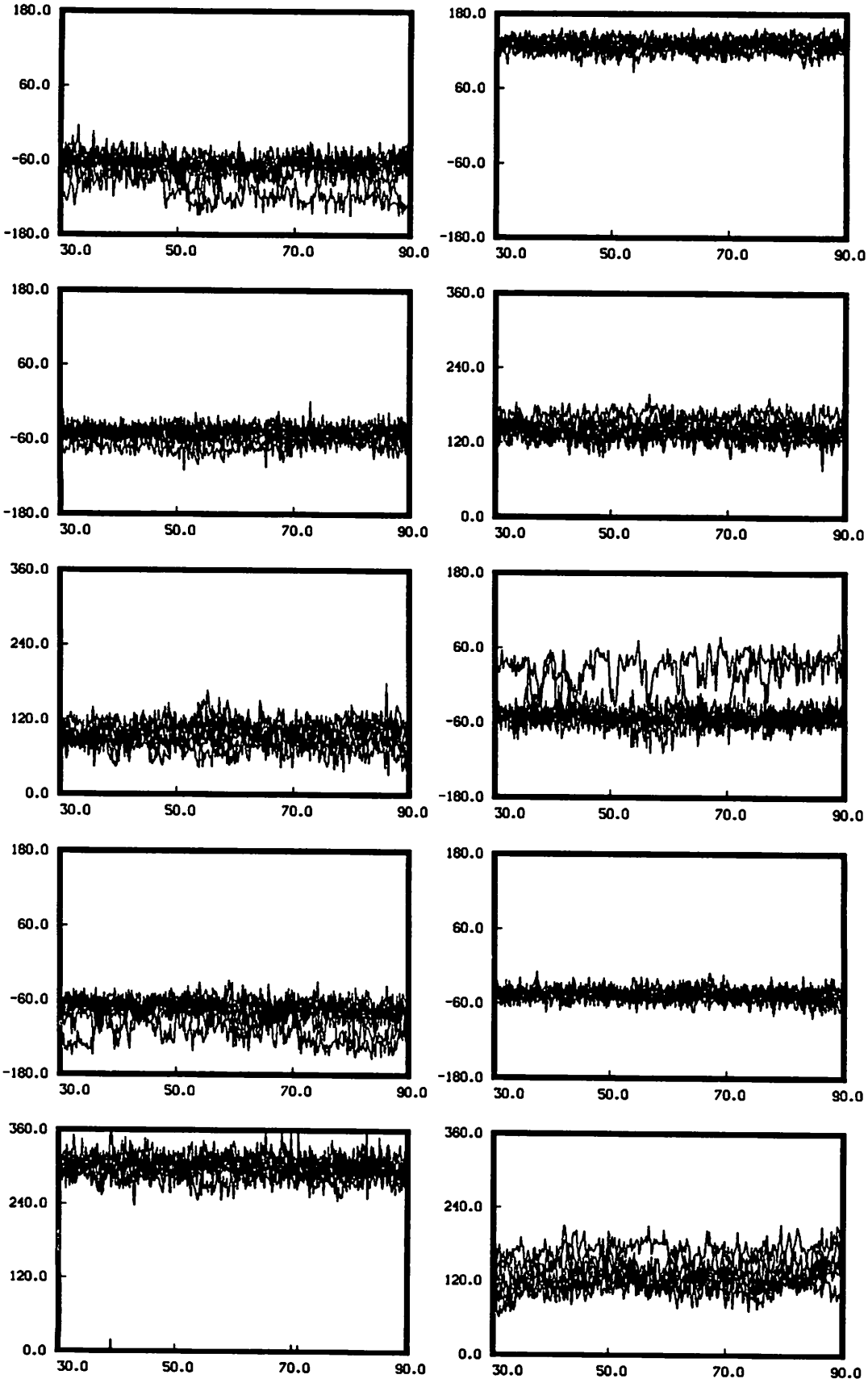

Figure 6. (*Continued*)

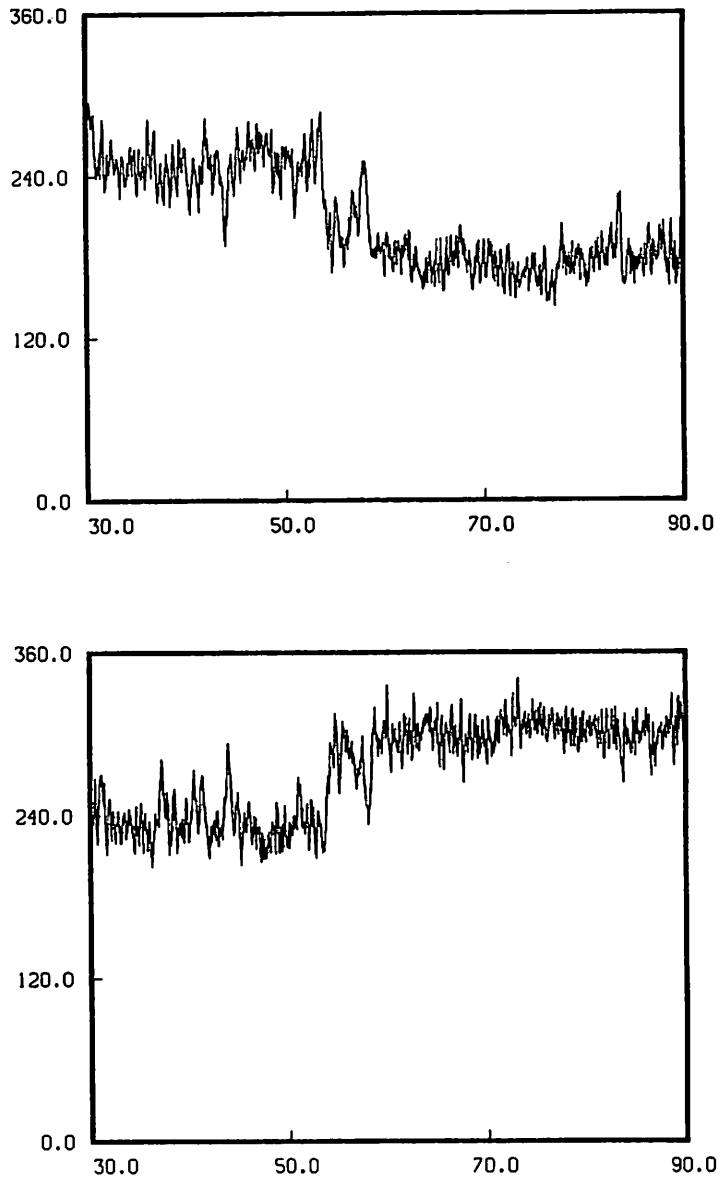

Figure 7 Histories of backbone angles ψ Gly_{35} (a) and ϕ Val_{36} (b) in simulation C. At about 54 ps, these angles experienced sharp counterrotations of about 90°, effecting a reorientation of the connecting peptide unit.

S_i may be accumulated separately, as shown in Table III. If crankshafting were an important mode in the thermal motion of the elastin polypentapeptide, we would expect S_i to be greater when calculated using $b = 0$ than using $b = 1$ when the motion of the ith and $(i - 1)$st bonds were correlated, and approximately equal when the rotations were uncorrelated. Table III shows that for conformation C correlated motions exist around all the peptide units except those connecting Val_1 and Pro_2, where the pyrrolidine ring of the proline imposes severe restrictions on the flexibility. In the more extended conformation D correlated motions are found only in the β-bend portion of the pentapeptide, where the variation in dihedral angles, and hence the number of conformations sampled, is small. It appears as though correlated counterrotations of ψ_i and ϕ_{i+1}, resulting in reorientation of the peptide units of the portions of the structure bridging β-bends, make an important contribution to the entropy of the relaxed state of elastin.

Surface Area Variations

Table IV lists values of the solvent-accessible surface areas[37] for the various structures as computed with

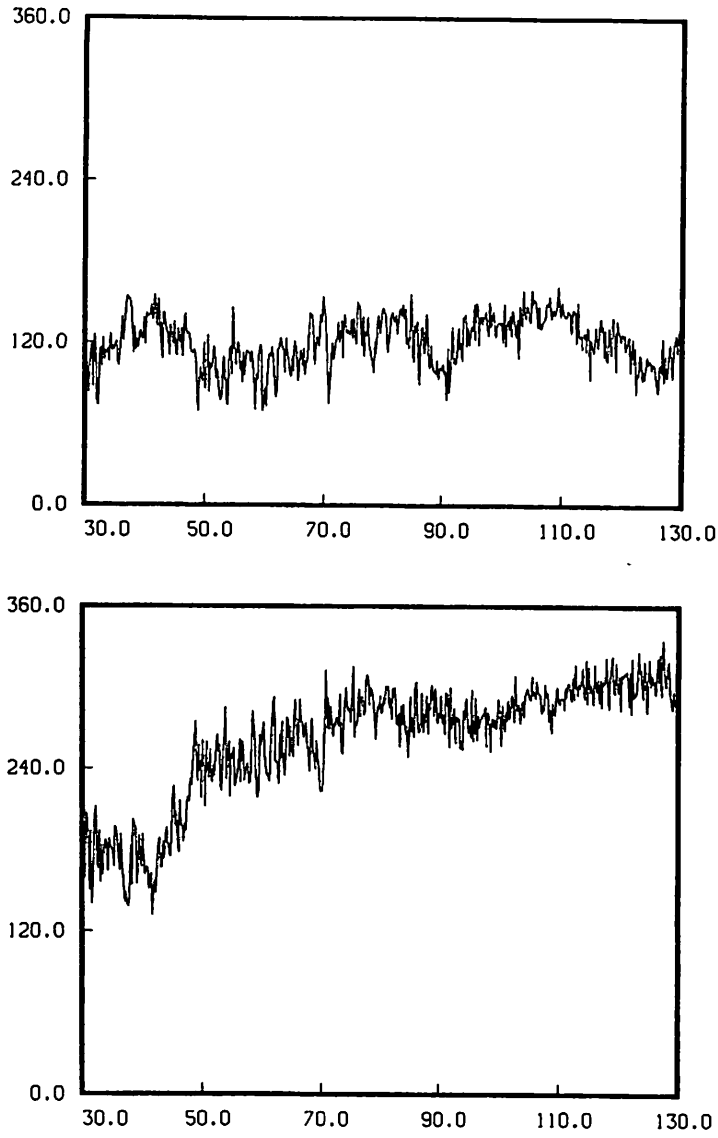

Figure 8 Histories of angles ψ Val_{39} (a) and ϕ Gly_{40} (b) of simulation B. Variations of the former angle were confined within a 40° range, whereas the latter angle underwent a gradual transition from *trans* to *gauche*$^+$. Several similar independent rotations in different parts of the structure took place during this simulation, causing severe deformations including the loss of two of the β-bends.

	S 1	S 2
S 1	1/4	1/4
S 2	1/4	1/4

a

	S 1	S 2
S 1	0	1/2
S 2	1/2	0

b

Figure 9 Probability matrix for a hypothetical molecule with only two rotatable bonds. Each bond has probability 1/2 of being found in either of the states S1 and S2. (a) The probability matrix corresponding to independent states of the two bonds, and (b) for anticorrelated states.

the Connolly algorithm[38] using a 1.4 Å probe sphere. Surfaces of the central eight pentapeptide units were computed every 10 ps, and the tabulated numbers are the averages, with standard deviations given in parentheses. The surface area of model C, the one with the smallest pitch, is several hundred square Ångstroms less than any of the others, indicating van der Waals interactions between atoms in successive turns of the spiral. Once the spiral has opened up enough for solvent molecules to penetrate between turns there is little change in surface area on further extension, and the area of models A, B, and D is similar to that of a fully extended all-*trans* chain.

Table III Entropy Contributions from Individual Angles

	Val-1		Pro-2		Gly-3		Val-4		Gly-5	
	ϕ	ψ	ϕ	ψ	ϕ	ψ	ϕ	ψ	ϕ	ψ
C $b = 0$	1.87	1.61	1.54	1.71	1.89	1.82	1.81	1.79	1.99	2.00
$b = 1$	1.75	1.58	1.52	1.70	1.78	1.79	1.72	1.75	1.87	2.03
D $b = 0$	1.78	1.50	1.60	1.68	1.75	1.83	1.75	1.49	1.70	1.84
$b = 1$	1.76	1.48	1.58	1.58	1.60	1.74	1.59	1.48	1.69	1.79

DISCUSSION

Structural and Dynamic Properties of Elastin

The structural and dynamical behavior of the elastin polymer differs in several respects from that generally observed in globular proteins. In the latter structures the polypeptide chain folds with a large change in solvent-accessible surface area to produce a compact globule whose interior is highly organized through extensive hydrogen bonding. Although substantial motion occurs in the surface loops of globular proteins,[39] the longer range, H-bonded interactions tend to keep the globular structure intact. Elastin, in contrast, incorporates only locally hydrogen-bonded β-turns, and so tends to writhe and drift during simulations, a reflection of the nondirectionality of the van der Waals interactions and hydrophobic forces that might otherwise tend to compact the structure.

We felt it remarkable that averaging dynamical motions of the relaxed structure should produce a regular model with near threefold symmetry (Figure 2). We take this to reflect the existence of stable threefold spirals that are closer in some respects to the cyclic pentapeptide crystal structure and have lower energy (Table I) than the original Urry spiral model. Assembly of 3 threefold spirals could potentially allow the formation of a twisted fibril with dimensions similar to those seen in electron microscopy (ca. 50 Å diameter).[40] Moreover, such fibrils would preserve many of the favorable intermolecular interactions seen in the cyclic pentadecapeptide crystal, locating solvent molecules exclusively in the spiral interior as with the cyclic molecules. What effect this would have on the librational motions observed here is not clear.

These fibrils would probably be characterized by a longer superspiral pitch for the individual chains than inferred for previous models[29] derived on the basis of electron microscope and diffraction features. However, it is possible that these features represent surface ridges or grooves in the triple-strand fibril that do not necessarily represent the pitch of individual polypentapeptide spirals. These are aspects of elastin structural assembly that deserve further investigation.

In this connection, the simulation of structure B, which lacked approximate threefold symmetry and was generally ill-behaved, seems to suggest that that organization into the higher order fibrillar structures may provide important, if not critical, reinforcement to spiral regularity. This appears to be an important correlate to the generation of librational entropy differences during elastin stretching, as apparent in the difference between the simulations of structures B and D (Table I).

Table IV Surface Area (sq. Ångstroms)

	Total	Polar
C	2083 (80)	616 (55)
A	2504 (39)	787 (25)
D	2501 (29)	683 (22)
B	2662 (40)	845 (35)
All-*trans*	2679	839

Librational and Hydrophobic Contributions to Elastin Entropy

The librational entropy model of elasticity proposed by Urry was originally based on molecular mechanics calculations for a single pentapeptide in relaxed and stretched conformations. These studies focused on the librational freedom of the segments bridging adjacent β-turns and showed that there were an increased number of low-energy unstretched conformations compared with low-energy stretched ones. More specifically, it was noted that rotations in ϕ_i, ψ_{i+1} angle pairs of the bridging segments Val_4-Gly_5-Val_1 were highly (anti)correlated. This was illus-

trated by λ plots of ψ_i vs ϕ_{i+1} in which the points corresponding to the low-energy conformations fall on a line of slope −1.[41]

It is of interest to ask to what extent the behavior inferred from the molecular mechanics model, which incorporates rigid bond lengths and angles, is present in the molecular dynamics simulations that incorporate more flexible geometry. In fact, basic features of the molecular dynamics and mechanics models are remarkably similar, as can be seen from Figure 10, which recasts the data of Figure 7 as a λ plot. In the plot, ψ_i, ϕ_{i+1} pairs are plotted every .2 ps, with the points before time 54 ps denoted by solid circles and those after 54 ps by x's. The effect of the correlated rotations, or cranklike motions, of Figure 7 is manifest in the points from the early part of the trajectory (solid circles) falling at the lower right, and those from the latter part of the trajectory (x's) at the upper left. The interesting observation is that the total collection of states does not form an equally populated continuum, so that the groups oscillate about one local librational state and then hop to another after 54 ps. Although many components of angular motion are altered when elastin is stretched, as described above in the Results, it is these state-switching crankshaft motions that seem to change most significantly on elastin stretching, and thus appear as important components of the elastomeric restoring force.

Recently Chang and Urry have published a report of a simulation of relaxed and extended states of the elastin polypentapeptide in vacuo.[20] They consider their polymer, seven pentapeptide units in length, to contain two units which are free of end effects. They report rms fluctuation in backbone angles ϕ and ψ that are somewhat smaller than those reported here (Table II), although this is probably the result of their averaging only over time within a single pentapeptide. Nevertheless, large rms deviations in linkages corresponding to ψGly_5-ϕVal_1 are observed that may suggest the occurrence of crankshaft motions of the sort described in Figure 7.

In the present simulation, the correlated counterrotations of ψ_i and ϕ_{i+1} that result in rotation or libration of the peptide bonds is much more pronounced for the relaxed molecules than for the extended ones, effecting a decrease in calculated entropy of about 1 cal/mol deg when the protein is stretched to 1.75 times its original length. Again, this value is similar to that obtained by Urry based

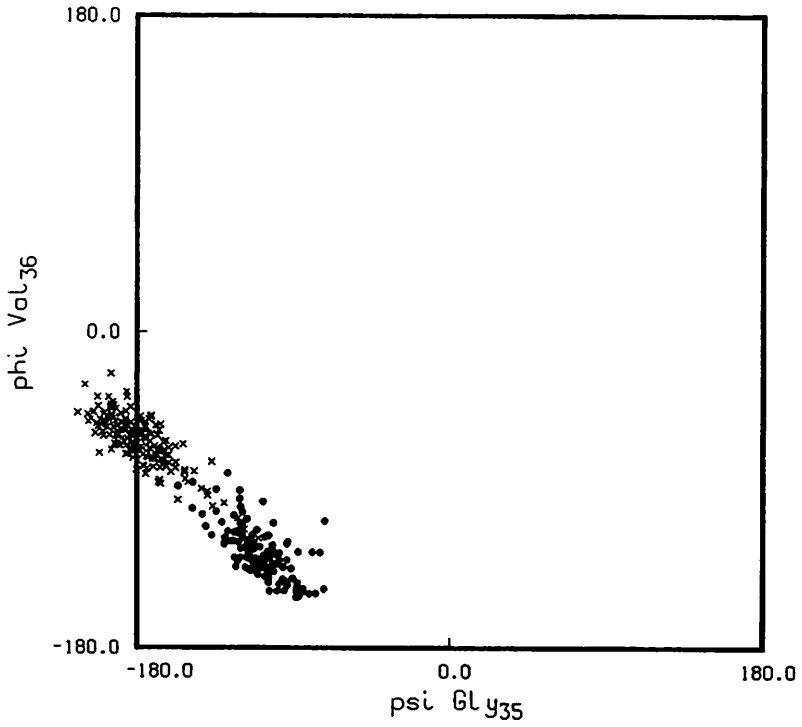

Figure 10 Lambda plots showing the variation in ψ Gly_{35} and ϕ Val_{36} during computer simulation C. Solid circles represent times from 30 to 54 ps, x's from 54 to 90 ps. Points are plotted every .2 ps. The migration from lower right to upper left indicates that a rotation of the peptide bond connecting Gly_{35} and Val_{36} has occurred.

on the number of low-energy pentapeptide conformations sampled by molecular mechanics calculations.[42] We conclude that the increased frequency and magnitude of these correlated rotations in the collapsed form of the polymer, relative to those in the stretched form, are at least partly responsible for the increased entropy of unstretched elastin, and hence its elasticity.

Another potential contributor to elastin elasticity is the hydrophobic effect. Since the water surrounding exposed hydrophobic side chains is rotationally and translationally ordered relative to bulk water,[43] it has been postulated that the extended forms of elastin that have greater hydrophobic surface area will have reduced (system) entropy. Experimental evidence for this proposal comes from several studies that show large changes in polymer hydration with stretching. Gosline[19] suggests that the hydrophobic effect is responsible for the decrease in entropy at low extension (less than 30%) and that conformational entropy is the major factor at higher extension. Although we have not made a detailed analysis of water mobility near the polymer on stretching that might ultimately be related to the hydrophobic effect, the simple variations in solvent-accessible surface area as the polymer is stretched substantially agree with Gosline's proposal. Simulation A has a smaller hydrophobic surface area than the more extended C (Table IV) although the calculated entropy is the same for both models. In contrast, structures C and D differ in conformational entropy, but have similar surface areas.

Note added in proof: Recent solution NMR studies of elastin polypentapeptide (44) suggest a coil conformation with approximately 2.9 pentapeptides per turn. This value is close to the near integral values of 3 pentapeptides per turn found in the averaged dynamic structure (Table I, Structure A) and used in subsequent simulations.

We are most grateful to Hagai Meirovich for making available his program to calculate the entropy of a protein from the results of a computer simulation, and to both him and Michael Levitt for useful discussions.

REFERENCES

1. Foster, J. A., Bruenger, E., Gray, W. R. & Sandberg, L. B. (1973) *J. Biol. Chem.* **248,** 2876–2879.
2. Sandberg, L. B., Soskel, N. T. & Leslie, J. G. (1981) *N. Engl. J. Med.* **304,** 566–579.
3. Bressan, G. M., Argos, P. & Stanley, K. K. (1987) *Biochemistry* **26,** 1497–1503.
4. Flory, P. J. (1953) *Principles of Polymer Chemistry,* Cornell University Press, Ithaca, New York.
5. Hoeve, C. A. J. & Flory, P. J. (1974) *Biopolymers* **13,** 677–686.
6. Dorrington, K. L. & McCrum, N. G. (1977) *Biopolymers* **16,** 1201–1222.
7. Andrady, A. L. & Mark, J. E. (1980) *Biopolymers* **19,** 849–855.
8. Urry, D. W., Wood, S. A., Harris, R. D. & Prasad, K. U. (1985) in *Polymers as Biomaterials,* Shalaby, S. W., Horbett, T., Hoffman, A. S. & Ratner, B., Eds., Plenum Publishing Co., New York, pp. 17–32.
9. Urry, D. W., Trapane, T. L. & Prasad, K. U. (1985) *Biopolymers* **24,** 2345–2356.
10. Urry, D. W., Haynes, B. & Harris, R. D. (1986) *Biochem. Biophys. Res. Commun.* **141,** 749–755.
11. Urry, D. W. (1986) in *Biomolecular Stereodynamics III,* Sarma, R. H. & Sarma, M. H., Eds., Adenine Press, New York, pp. 173–196.
12. Urry, D. W., Henze, R., Harris, R. D. & Prasad, K. U. (1984) *Biochem. Biophys. Res. Commun.* **125,** 1082–1088.
13. Urry, D. W., Henze, R., Redington, P., Long, M. M. & Prasad, K. U. (1985) *Biochem. Biophys. Res. Commun.* **128,** 1000–1006.
14. Urry, D. W., Trapane, T. L., Iqbal, M., Venkatachalam, C. M. & Prasad, K. U. (1985) *Biochemistry* **24,** 5182–5189.
15. Urry, D. W., Trapane, T. L., McMichens, R. B., Iqbal, M., Harris, R. D. & Prasad, K. U. (1986) *Biopolymers* **25,** S209–S228.
16. Urry, D. W., Shaw, R. G. & Prasad, K. U. (1985) *Biochem. Biophys. Res. Commun.* **130,** 50–57.
17. Urry, D. W. (1988) *J. Protein Chem.* **7,** 1–34.
18. Gray, W. R., Sandberg, L. B. & Foster, J. A. (1973) *Nature* **246,** 461–466.
19. Gosline, John M. (1978) *Biopolymers* **17,** 677–695.
20. Chang, D. K. & Urry, D. W. (1988) *Chem. Phys. Lett.* **147,** 395–400.
21. Venkatachalam, C. M. & Urry, D. W. (1981) *Macromolecules* **14,** 1225–1229.
22. Cook, W. J., Einspahr, H., Trapane, T. L., Urry, D. W. & Bugg, C. E. (1980) *J. Am. Chem. Soc.* **102,** 5502–5505.
23. Urry, D. W., Trapane, T. L., Sugano, H. & Prasad, K. U. (1981) *J. Am. Chem. Soc.* **103,** 2080–2089.
24. Urry, D. W. & Long, M. M. (1976) *CRC Crit. Rev. Biochem.* **4,** 1–45.
25. Weiner, P. K. & Kollman, P. A. (1981) *J. Comp. Chem.* **2,** 287–303.
26. Weiner, S. J., Kollman, P. A., Case, D. A., Singh, U. C., Ghio, C., Alagona, G., Profeta, S. Jr. & Weiner, P. (1984) *J. Am. Chem. Soc.* **106,** 765–784.
27. Jorgensen, W. L., Chandrasekhar, J., Madura, J., Impey, R. W. & Klein, M. L. (1983) *J. Chem. Phys.* **79,** 926–935.
28. Prabhakaran, M. & Harvey, S. C. (1985) *J. Phys. Chem.* **89,** 5767–5769.

29. Urry, D. W. (1983) *Ultrastruct. Pathol.* **4**, 227–251.
30. Berendsen, H. J. C., Postma, J. P. M., van Gunsteren, W. F., DiNola, A. & Haak, J. R. (1984) *J. Chem. Phys.* **81**, 3684–3690.
31. Hilmer, R. M. (1989) *J. Mol. Graphics* **7**, 212–216.
32. Meirovitch, H., Vasquez, M. & Scheraga, H. A. (1987) *Biopolymers* **26**, 651–671.
33. Olson, W. K. (1981) in *Biomolecular Stereodynamics I*, Sarma, R. H. Ed., Adenine Press, New York, pp. 327–343.
34. Peticolas, W. L. & Kurtz, B. (1980) *Biopolymers* **19**, 1153–1166.
35. Helfand, E., Wasserman, Z. R. & Weber, T. A. (1980) *Macromolecules* **13**, 526–533.
36. Helfand, E. (1985) *J. Polymer Sci.* **73**, 39–54.
37. Lee, B. K. & Richards, F. M. (1978) *J. Mol. Biol.* **55**, 379–400.
38. Connolly, M. L. (1983) *Science* **221**, 709.
39. Salemme, F. R., Genieser, L., Finzel, B. C., Hilmer, R. M. & Wendoloski, J. J. (1988) *J. Crystal Growth* **90**, 273–282.
40. Urry, D. W. (1978) *Perspect. Biol. Med.* **21**(2), 265–295.
41. Urry, D. W. & Venkatachalam, C. M. (1983) *Int. J. Quant. Chem. Quant. Biol. Symp.* **10**, 81–93.
42. Urry, D. W. (1984) *J. Protein Chem.* **3**, 403–436.
43. Levitt, M. & Sharon, R. (1988) *Proc. Natl. Acad. Sci. USA*, **85**, 7557–7561.
44. Chang, D. K., Venkatachalam, C. M., Prasad, K. U., Urry, D. W., (1989) *J. Biomolec. Structure and Dynamics* **6**, 851–858

Received May 16, 1989
Accepted October 4, 1989